Outer Billiards, Arithmetic Graphs and Multigrid Flows

Richard Evan Schwartz *

January 22, 2012

1 Introduction

This is an informal research note which contains statements of results, but no proofs. The purpose of the note is to describe a *coarse isomorphism* I discovered between two seemingly different dynamical constructions, namely

1. The *arithmetic graphs* associated to outer billiards on kites.

2. The *multigrid flow*, defined on certain *decorated multigrids*.

I considered the first construction in my book, *Outer Billiards on Kites* [**S2**]. The *arithmetic graphs* served as the main tool for understanding the dynamics of outer billiards on kites. See §2 for definitions. The second construction, which is quite general, is based on patterns of oriented lines in the Euclidean plane. See §3 for definitions.

The concrete instance of the multigrid construction that is related to outer billiards on kites is closely connected to *Sturmian sequences*. I am grateful to John Smillie for his beautiful explanation of the renormalization theory for Sturmian sequences. I am also grateful to Smillie (and also Mark Sapir) for suggesting to me that my arithmetic graphs might be related to Sturmian sequences. This connection is far from being worked out.

I call my main result the Coarse Isomorphism Theorem. I have not yet tried to prove the Coarse Isomorphism Theorem, though I have some idea

* Supported by N.S.F. Research Grant DMS-0072607

of how it will be done. The Coarse Isomorphism Theorem is supported by massive computer evidence. I will amply illustrate this note with examples, taken from the computer program I wrote.

The Coarse Isomorphism Theorem allows one to essentially reduce the study of outer billiards on kites to the study of certain multigrid flows. I have not yet tried to deduce corollaries from the Coarse Isomorphism Theorem, but I can see that the corollaries will be manifold. For instance, the multigrid flows defined here should enjoy a rich renormalization theory just as Sturmian sequences do.

The renormalization theory I have in mind should explain the kind of (coarse) self-similarity one sees in the arithmetic graphs associated to outer billiards on kites. In [**S1**] I established some coarse self-similarity properties of the arithmetic graphs associated to the Penrose kite, the kite that arises in the Penrose kites-and-darts tilings. Similar results should hold for any *quadratically irrational kite*, but the methods in [**S1**] and [**S2**] are not powerful enough to reach these results. The Coarse Isomorphism Theorem promises to be an effective tool for this.

Naturally, I intend to prove the Coarse Isomorphism Theorem, and also to study the structure of the associated multigrid flows. However, I imagine that the various proofs involved will be rather extensive. For now, I just want to state the main result clearly.

Here is an outline of this note. In §2, I will recall the definition of the *arithmetic graph*. In §3, I will define what I mean by the *multigrid flow*. I will also describe the concrete examples that arise in the Coarse Isomorphism Theorem. In §4 will define what I mean by a *coarse isomorphism*, and I will state two versions of the main result.

2 Arithmetic Graphs

2.1 Polygonal Outer Billiards

To define a polygonal outer billiards system, one starts with a convex polygon $P \subset \boldsymbol{R}^2$. Consider a typical point $x_0 \in \boldsymbol{R}^2 - P$. One defines x_1 to be the point such that the segment $\overline{x_0 x_1}$ is tangent to P at its midpoint and P lies to the right of the ray $\overrightarrow{x_0 x_1}$. The iteration $x_0 \to x_1 \to x_2 ...$ is called the *forwards outer billiards orbit* of x_0.

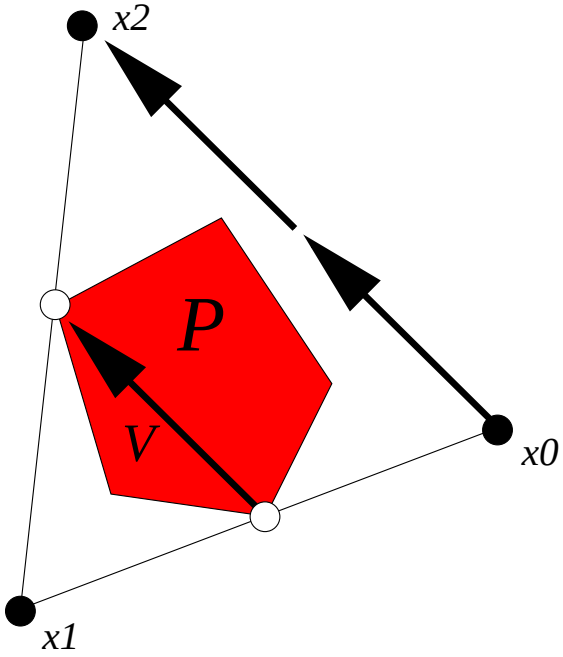

Figure 1.1: outer billiards relative to P.

We denote the outer billiards map relative to P by ψ', and the square of the outer billiards map by $\psi = (\psi')^2$. These maps are defined away from a countable set of line segments in $\boldsymbol{R}^2 - P$.

We have the equation

$$\psi(x_0) - x_0 = 2V. \tag{1}$$

Here V is a vector that points from one vertex of P to another. The choice of V depends on x_0. The map ψ is a local translation. Equation 1 is the starting point for the definition of the arithmetic graph.

2.2 Outer Billiards on Kites

A *kite* is a convex quadrilateral such one of the diagonals is a line of symmetry. Each kite is affinely equivalent to the kite $K(A)$ with vertices

$$(-1,0); \qquad (0,1); \qquad (0,-1); \qquad (A,0); \qquad A \in (0,1]. \tag{2}$$

The case $A = 1$ corresponds to the square. We ignore this case and take $A \in (0,1)$. Outer billiards is an affinely natural dynamical system, so the study of outer billiards on kites reduces to the study of outer billiards on various $K(A)$.

We will work entire with the square-map ψ. We define Λ to be the set of points in $\boldsymbol{R}^2$ of the form $(2Am + 2n, 2o)$, where

- $(m,n,o) \in \boldsymbol{Z}^3$;
- $m + n + o$ is even.

Examining the possible vectors in Equation 1, for the case of $K(A)$, we get $\psi(p) - p \in \Lambda$. Hence the coset $\Lambda + \theta$ is invariant under ψ for any $\theta \in \boldsymbol{R}^2$. For almost all choices of θ, the map ψ is entirely defined on $\Lambda + \theta$. We always work with such θ.

We want to study how ψ permutes $\Lambda + \theta$. Given the definition of Λ, it suffices to consider the case when $\theta \in [0,2] \times [-1,1]$. Reflection in the x-axis conjugates ψ to ψ^{-1}. Thus, the orbit of (x,y) is conjugate to the orbit of $(x,-y)$, and it suffices to consider the case when $y \geq 0$. For these reasons, we will always take

$$\theta \in [0,2] \times [0,1] \tag{3}$$

when we consider the dynamics of ψ on $\Lambda + \theta$. Figure 2.2 shows $K(A)$, for $A = 1/2$, as well as the rectangle $[0,2] \times [0,1]$.

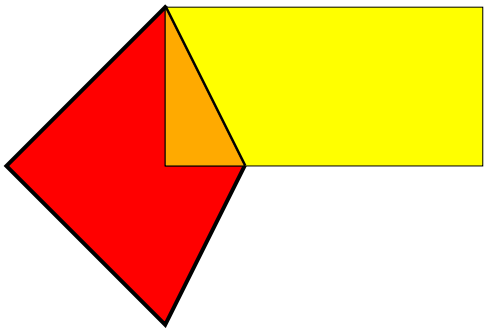

Figure 2.2: $K(1/2)$ and the rectangle $[0,2] \times [0,1]$.

2.3 The Arithmetic Graph

Now we describe the construction of the *arithmetic graph*. This construction is related to the *lattice vector fields* studied by Vivaldi et. al. in [**VL**]. First we will describe a general construction, and then we will modify/specialize the construction to suit our purpose of studying outer billiards on kites. We work exclusively with the square-map, ψ. Let P be a convex polygon, as above, with vertices $V_1, ..., V_n$. Let $\boldsymbol{A}$ denote the $\boldsymbol{Z}$-module of formal linear combinations of the form

$$\sum a_{ij} V_{ij}; \qquad V_{ij} = V_i - V_j; \qquad a_{ij} \in \boldsymbol{Z}.$$

As in Equation 1, the square of the outer billiards map is a translation by $2V_{ij}$ for some pair of indices. Thus, one can consider outer billiards orbits formally as paths in $\boldsymbol{A}$. This is the general idea. Now we specialize to the case of kites.

Let $\theta = (x_0, y_0) \in [0,1] \times [0,2]$. Define

$$\Xi_\theta = \Xi_\theta^+ \cup \Xi_\theta^-;$$

$$\Xi_\theta^+ = \{(x,y) |\ x > 0;\ \ y = y_0\};$$
$$\Xi_\theta^- = \{(x,y) |\ x > 0;\ \ y = y_0 - 2\}. \tag{4}$$

Then Ξ_θ is the union of 2 rays. The most symmetric case occurs when $y_0 = 1$. In this case, $\Xi_+ = \boldsymbol{R}_+ \times \{-1, 1\}$.

Our constructions rely on the following lemma, which we will just assume here.

Lemma 2.1 (Return Lemma) *For any point $q \in \Xi_\theta$, with a well-defined orbit, there are points $\theta_-, \theta_+ \in \Xi_\theta$ such that θ_- lies in the backward orbit of θ and θ_+ lies in the forward orbit of θ.*

In [**S2**], we proved this result when $\theta = (x_0, 1)$, but the general case is essentially the same. The Return Lemma allows us to define the first return map $\Psi : \Xi_\theta \to \Xi_\theta$.

Consider the affine map

$$\tau(x,y) = 2Ax + 2y + x_0 \tag{5}$$

Let

$$H = H_{A,\theta} = \tau^{-1}(\boldsymbol{R}_+). \tag{6}$$

We consider H to be an open halfplane, except that we include $(0,0)$ in H. On $H \cap \boldsymbol{Z}^2$, we define

$$T(m,n) = \theta + \Big(\tau(x,y), y_0 - 1 + (-1)^{m+n}\Big) \tag{7}$$

By construction, T is a bijection from $H \cap \boldsymbol{Z}^2$ to $\Xi_+ \cap \Lambda_\theta$. Now we define the arithmetic graph as follows. Two points (m_1,n_1) and $(m_2,n_2) \in \boldsymbol{Z}^2 \cap H$ are joined by a directed edge iff

$$\Psi \circ T(m_1,n_1) = T(m_2,n_2). \tag{8}$$

The arithmetic graph is a directed graph. We call this graph $\widehat{\Gamma}(\theta;A)$. The components of $\widehat{\Gamma}(\theta;A)$ correspond bijectively with the orbits of ψ on Λ_θ. The component $\Gamma(\theta;A)$ containing $(0,0)$ corresponds to the orbit of θ. Here we will assume the following result.

Theorem 2.2 (Embedding) *The graph $\widehat{\Gamma}(\theta;A)$ is a disjoint union of embedded polygons and embedded infinite polygonal arcs. Moreover, each edge of $\widehat{\Gamma}(\theta;A)$ joins a point in $\boldsymbol{Z}^2$ to one of its 8 nearest neighbors.*

In [**S2**] we proved the embedding theorem in case $y_0 = 1$. The proof in the general case is similar, though we have not written down a proof. The proof is rather complicated. We don't actually use the Embedding Theorem for any purpose in this note, but it is a nice result to keep in mind.

The Temperature: Let $\theta = (x_0, y_0)$. We define the *temperature* of $\widehat{\Gamma}(\theta;A)$ to be y_0. Then the temperature of $\widehat{\Gamma}(\theta,A)$ varies between 0 and 1. In [**S2**] we made a very detailed study of the graphs of temperature 1. In the next section, we will focus on how the graphs change as the temperature drops from 1 to 0. This study will lead naturally to the description of our multigrid flows.

The Rational Case: We can define $\widehat{\Gamma}(\theta,A)$ even when A is rational, but then a bit of care must be taken. The slight technical problem is that T is not injective on $\boldsymbol{Z}^2$. However, T is injective on disks of radius q, and this suffices to define $\widehat{\Gamma}(\theta,A)$ as above. Let $A = p/q$. For each temperature y_0, there is some $\epsilon > 0$ such that $\widehat{\Gamma}(\theta,A)$ is independent of $\theta = (x_0,y_0)$ as long as $x_0 \in (0,\epsilon)$. The value of ϵ depends on $A = p/q$. For example, when $y_0 = 1$, the largest choice is $\epsilon = 2/q$. (When the temperature is 1, we set $\epsilon = 1/q$ for concreteness.) We will set $\widehat{\Gamma}(y_0,A) = \widehat{\Gamma}(\theta,A)$ for such values of ϵ. We let $\Gamma(y_0,A)$ denote the component of $\widehat{\Gamma}(y_0,A)$ that contains $(0,0)$.

2.4 Some Pictures

In [**S2**] we drew a great many pictures of $\Gamma(A,p)$ when $p=(x_0,1)$. For convenience, we will draw all out pictures relative to the parameter 17/72. This rational parameter is a close approximation to ϕ^{-3}, where ϕ is the golden ratio. The kite $K(\phi^{-3})$ has some special significance. It is affinely equivalent to the Penrose kite. We studied outer billiards on the Penrose kite in [**S1**] as a prelude to [**S2**].

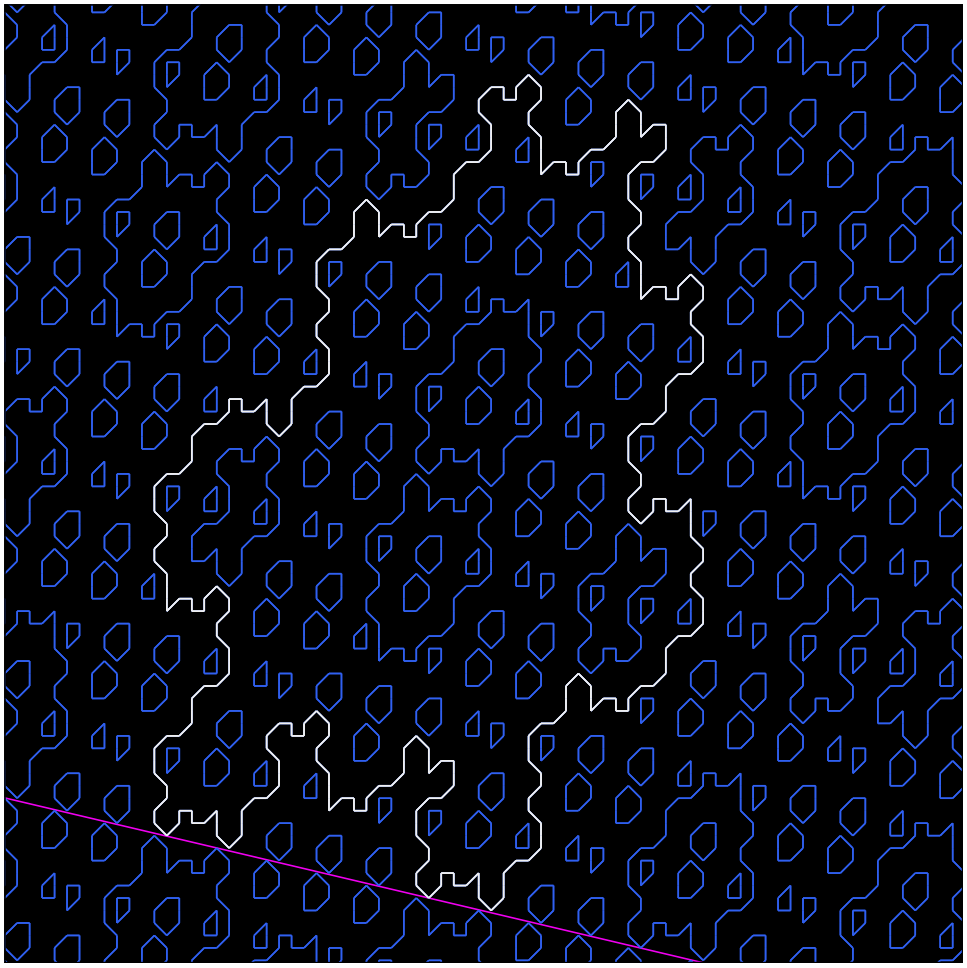

Figure 2.3: $\widehat{\Gamma}(1,17/72)$ in blue and $\Gamma(1,17/72)$ in white.

The pink line in Figure 2.3 is ∂H. We have just defined $\widehat{\Gamma}$ on $\boldsymbol{Z}^2 \cap H$, but in fact there is a canonical extension to all of $\boldsymbol{Z}^2$. Our pictures show this extension.

Now we start dropping the temperature. Figure 2.4 shows the temperature $y_0 = 8/21$. Since $y_0 < 1$, the component containing $(0, 0)$ is trivial. (The corresponding point (ϵ, y_0) lies inside $K(A)$ in this case. So, we show some other interesting component.

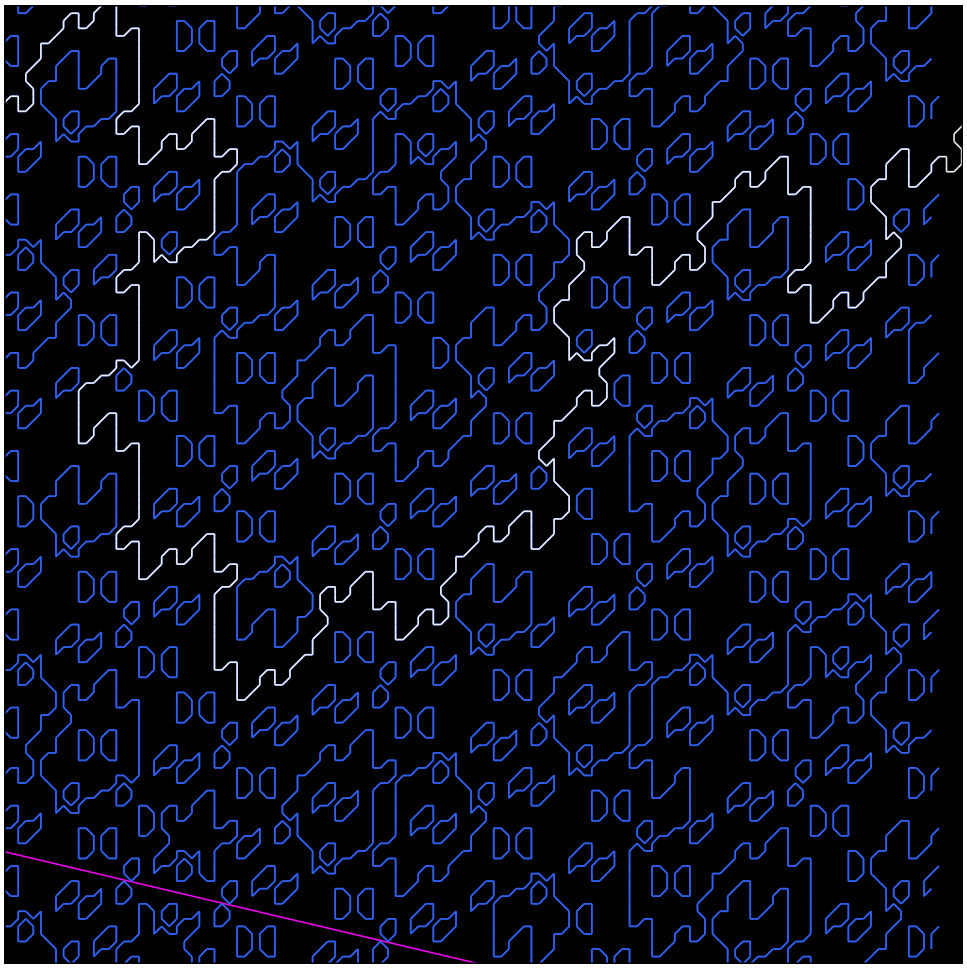

Figure 2.4: $\widehat{\Gamma}(8/21, 17/72)$ in blue and some component of $\widehat{\Gamma}(8/21, 7/72)$ in white.

The reader can perhaps see the hint of a "grid" in Figure 2.4. As we drop the temperature further, the grid becomes more obvious. Figure 2.5 shows the case when the temperature is 8/55. (In the spirit of the example, we are choosing temperatures that are ratios of Fibonacci numbers.)

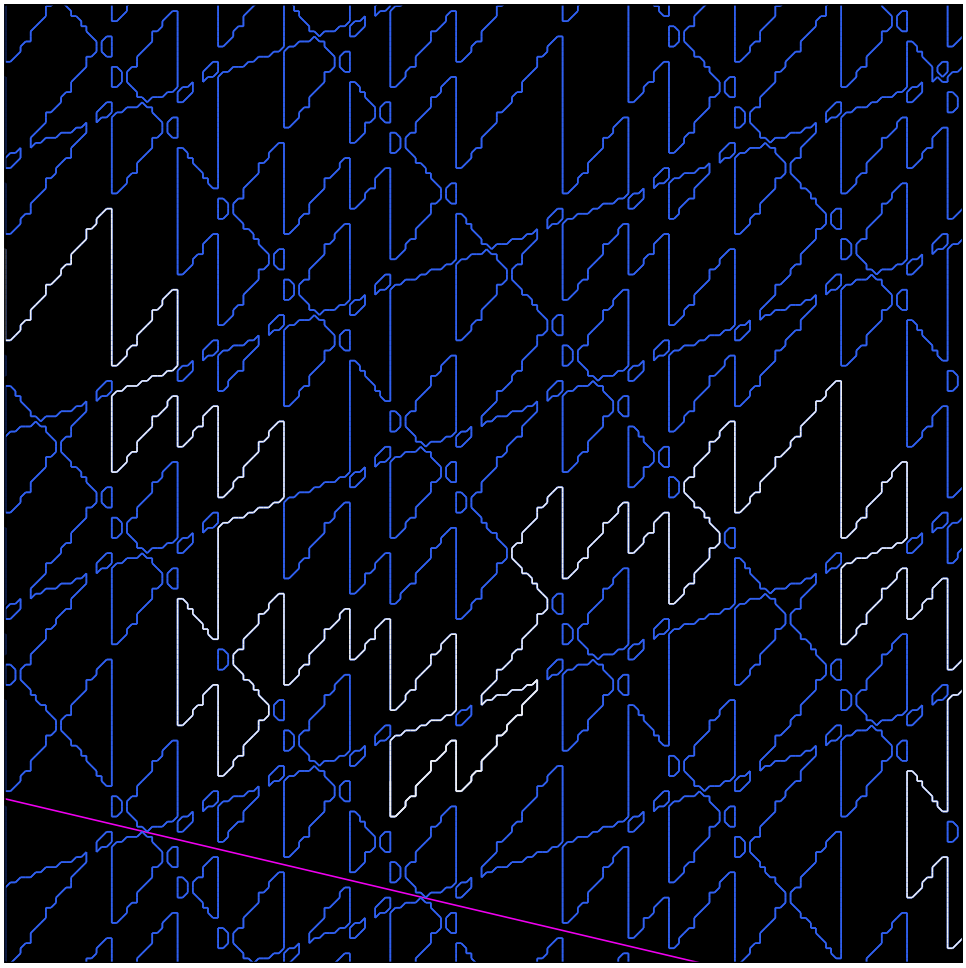

Figure 2.4: $\widehat{\Gamma}(8/55, 17/72)$ in blue and some component of $\widehat{\Gamma}(8/21, 7/72)$ in white.

Looking at the figure, we see the following kind of structure emerge. There seems to be an underlying grid of lines. The orbits essentially follow along these lines until they reach an intersection. Having reached an intersection, the orbits turn onto a new line.

As the temperature drops to 0, the grid becomes more and more obvious. Experimentally, we analyzed the picture carefully for temperatures near 0 and discovered the structure of the grid. Somewhat surprising, there is an underlying grid at all temperatures, though it is obscured by local fluctuations which are negligible at low temperatures. Our Coarse Isomorphism Theorem will make all this more precise.

3 Multigrid Flows

3.1 The Basic Definition

We say that a *multigrid* is a locally finite union $\mathcal{G}$ of oriented lines in the plane. The local finiteness condition means that every compact set intersects only finitely many lines. Usually, we assume that the lines are in general position, meaning that no three are coincident. We say that a *decoration* of $\mathcal{G}$ is a 2-coloring of the intersection points of the lines of $\mathcal{G}$. We call a vertex either *decorated* or *plain*. We will draw the decorated vertices as dots, and we will do nothing for the plain vertices.

Say that a unit speed arc in $\mathcal{G}$ (that is contained on a single line) *obeys the law* if it follows along the orientation of the line. Say that such an arc *breaks the law* if it goes against the orientation. Naturally, we have in mind cars driving along a system of one-way roads.

Let x be a point of $\mathcal{G}$ that does not lie on an intersection point. Then we can define two polygonal arcs starting at x. We call these the *forward arc* and the *backward arc*. We will describe the forward arc. We move along the line containing x, obeying the law, until we reach an intersection. If the intersection is plain, we turn onto the new line, so as to obey the law. If the intersection if decorated, we turn so as to break the law. In general, we do one of 4 things at an intersection.

- If we are obeying the law and we reach a plain intersection, we turn so as to obey the law.
- If we are breaking the law and we reach a plain intersection, we turn so as to break the law.
- If we are obeying the law and we reach a decorated intersection, we turn so as to break the law.
- If we are breaking the law and we reach a decorated intersection, we turn so as to obey the law.

In short, we turn at every intersection. At a plain vertex, we continue in our current state with respect to the law, and at a decorated vertex we switch states.

In the special case when all the intersections are plain, the forward arc moves so as to always obey the law, and the backward arc moves so as to always break the law.

The union of the forward and backward arcs through x is what we call the *grid orbit* of x. This union is either a closed polygon or else an infinite polygonal arc. This polygon is not necessarily embedded, but it never crosses itself. That is, the grid orbit has arbitrarily small perturbations that are embedded. Figure 3.1 shows an example, based on 3 oriented lines. We have given different colors to the 3 grid orbits. We have also added numbers to indicate the path traced out by the yellow orbit. In this example, the orbits travel out to infinity in the obvious way.

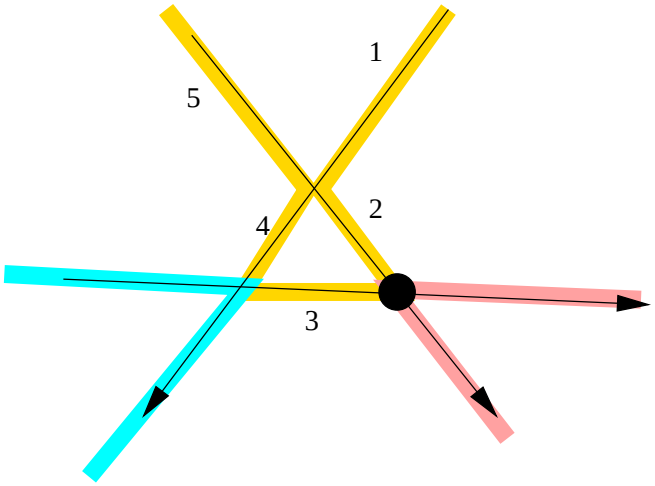

Figure 3.1: Grid Orbits

3.2 Sturmian Grids

We will now describe an infinite union $\mathcal{U}(c_1, c_2, c_3, \lambda, \sigma, \epsilon)$ of oriented lines in the plane. Here

- $c_1 < 1/2$ determines a locally affine map from $\boldsymbol{Z}$ to $\boldsymbol{R}/\boldsymbol{Z}$.
- c_2 determines the radius of an interval in $\boldsymbol{R}/\boldsymbol{Z}$.
- c_3 determines the center point of the same interval.
- $\lambda \in [0, 1)$ is a number we call the *offset*.
- $\sigma \in (0, 1]$ is a number that determines the slopes of our lines.
- $\epsilon \in \{-1, 1\}$ is a bit that determines the way we orient the lines.

Here is the construction. Let $n \in \boldsymbol{Z}$. Let $[c_1(n+\lambda)]$ be the class of $(c_1+\lambda)n$ in $\boldsymbol{R}/\boldsymbol{Z}$. If $[(c_1(n+\lambda)]$ lies within c_2 of the point $[c_3]$, then we include the two lines of slope $\pm\sigma$, based at the point $(n+\lambda, 0)$ in our union $\mathcal{U}$. Otherwise we do not. This gives us our family of lines in $\mathcal{U}$. It remains only to specify the orientations. If $\epsilon = 1$ we orient the lines of slope $-\sigma$ downward and the line of slope σ upward. If $\epsilon = -1$, we do the opposite. We call $\mathcal{U}$ a *Sturmian grid*.

Now suppose that $A \in (0,1)$ and $\theta = (x_0, y_0) \in [0,2] \times [0,1]$, as in the previous chapter. We are going to define $\mathcal{U}(A,\theta)$ to be the union of two Sturmian grids. Here we are parameters for the first grid.

- $c_{11} = (1-A)/2$.
- $c_{12} = y_0/4$.
- $c_{13} = (1+x_0)/4$.
- $\lambda_1 = 0$.
- $\sigma_1 = 1$.
- $\epsilon_1 = 1$.

Here are the parameters for the second grid.

- $c_{21} = (1-A)/2$.
- $c_{22} = (Ay_0)/4$.
- $c_{23} = (3+x_0)/4$.
- $\lambda_2 = 1/2$.
- $\sigma_2 = A$.
- $\epsilon_2 = -1$.

Given these parameters, we define

$$\mathcal{U}(\theta; A) = \mathcal{U}_1 \cup \mathcal{U}_2; \qquad \mathcal{U}_k = \mathcal{U}(c_{k1}, c_{k2}, c_{k3}, \lambda_k, \sigma_k, \epsilon_k). \tag{9}$$

3.3 Some Remarks

To anticipate the Coarse Isomorphism, we will see that the multigrid flow on $\mathcal{U}(\theta; A)$, when it is suitably decorated, produces a collection of orbits that is coarsely identical to the components of the arithmetic graph $\Gamma(\theta; A)$. In the next section we will explain how the decoration works.

Monotonicity: Before we get to the decoration of our multigrid, we discuss, in an informal way, what happens as the point θ varies. We are interested in revisiting the temperature dropping phenomenon discussed in the previous section. First of all, we have a certain monotonicity phenomenon. Let $\theta_1 = (x_0, y_1)$ and $\theta_2 = (x_0, y_2)$. Assume that $y_2 < y_1$. Then

$$\mathcal{U}(\theta_2; A) \subset \mathcal{U}(\theta_1; A).$$

This is immediate from the definitions. The only thing that happens when we change from θ_1 to θ_2 is that the corresponding intervals in $\boldsymbol{R}/\boldsymbol{Z}$ shrink about their midpoints. Considering the variable point $\theta = (x_0, y)$, we observe that the two intervals defining $\mathcal{U}(\theta; A)$ shrink to points as $y \to 0$.

General Position: There are several ways that our grid $\mathcal{U} = \mathcal{U}(\theta; A)$ could fail to be in general position. First of all, it might happen that at least 3 lines of $\mathcal{U}$ are coincident. For each choice of A, there is a 1-dimensional set of choices of θ which lead this situation. For ease of exposition, we assume that we have chosen θ to that these triple points do not occur.

Second of all, it might happen that some point $[c_{k1}n]$ is precisely c_{k2} units away from $[c_{k3}]$. Again, for fixed A, this happens for a 1-dimensional set of choices of θ. We will assume that θ is chosen so that the situation we have just discussed does not happen.

Our results still work even in these degenerate cases, but the situation is somewhat more difficult to describe. The situation is that our computer program is designed to handle all the exceptional cases, but we do not mention them here explicitly. We warn the reader in advance that sometimes we will draw pictures that contain degenerate cases. We like to draw pictures for rational parameters, and these tend to contain some degeneracies.

3.4 Decorations

Let $\mathcal{U} = \mathcal{U}_1 \cup \mathcal{U}_2$, as above. We draw the lines of $\mathcal{U}_1$ in blue and the lines of $\mathcal{U}_2$ in red. The blue lines have slope ± 1, and the read lines have slope $\pm A$. Here we explain which intersection points we decorate. We isolate a certain configuration of lines which we call a *k-ladder*. Figure 3.2 shows the cases $k = 1, 2, 3$. The pattern continues in the obvious way. A k-ladder can point in one of 4 directions. The bottom row of our picture shows 2 possibilities for a 3-ladder.

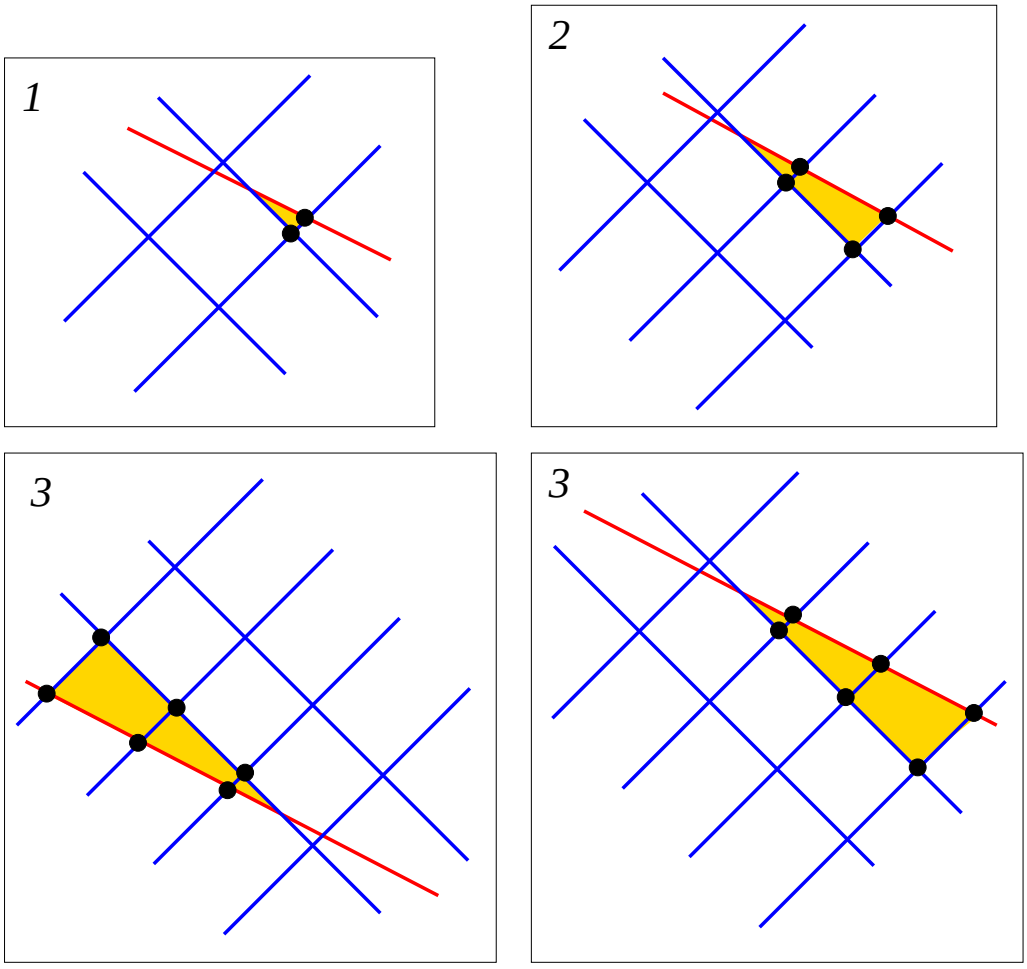

Figure 3.2: k-ladders for $k = 1, 2, 3$.

The blue lines involved in a latter are meant to be as close together as possible. That is, two consecutive blue lines intersect the x-axis in consec-

utive integers. Put another way, the blue squares involved in a ladder have unit length diagonals.

We decorate $2k$ of the vertices, as shown in Figure 3.2. We call these the *distinguished vertices* of the k-ladder. Our configurations are meant to be embedded inside a larger collection of lines. However, the ladder must be *embedded* in the sense that no additional line can intersect the yellow triangular regions defined by the ladder, as shown in Figure 3.2.

Decoration Rule: We decorate an intersection if and only if if it is one of the distinguished vertices of a ladder.

Let $\theta = (x_0, y_0)$, as above. Here we make some experimental observations about the decorations of $\mathcal{U}(\theta; A)$.

- The number of k-ladders in $\mathcal{U}(\theta; A)$ is monotone increasing as y_0 increases and x_0 is held fixed. More precisely, as we vary y_0 from 0 to 1, new ladders appear from time to time, but never disappear.

- When $y_0 < 1/(1 + A)$ there are no ladders in $\mathcal{U}(\theta; A)$. In this case, the grid consists entirely of plane vertices.

- For certain parameters, such as

  $$A = \sqrt{n^2 + 1} - \text{floor}(\sqrt{n^2 + 1}); \qquad n = 1, 2, 3...$$

  and

  $$A = 2\sqrt{n^2 + n + 1} - \text{floor}(2\sqrt{n^2 + n + 1}); \qquad n = 1, 2, 3...$$

  there are no ladders at all. Thus, again $\mathcal{U}(\theta; A)$, has only plain vertices. We note that the case $n = 2$ for the first family corresponds to the Penrose kite parameter $\sqrt{5} - 2$.

- When $A < 1/2$, there are never any k-ladders for $k \geq 2$. More generally, for any $\epsilon > 0$ there is some N such that there are no N-ladders provided that $A < 1 - \epsilon$. In other words, one only sees long ladders as $A \to 1$.

We don't completely understand what properties of the parameters causes the ladders to appear in the grid, but the decoration of the grid is crucial to our Coarse Isomorphism Theorem.

3.5 Some Pictures

Figure 3.3 shows part of $\mathcal{U}(\theta; A)$ for $\theta = (1/45, 1)$ and $A = 31/45$. We have shown all the visible decoration. One should be able to see two 2-ladders and one 1-ladder. Recall that the decorated points come in pairs. Some of the pairs are so close together that they appear as a single point. The clearest 2-ladder is in the upper left corner.

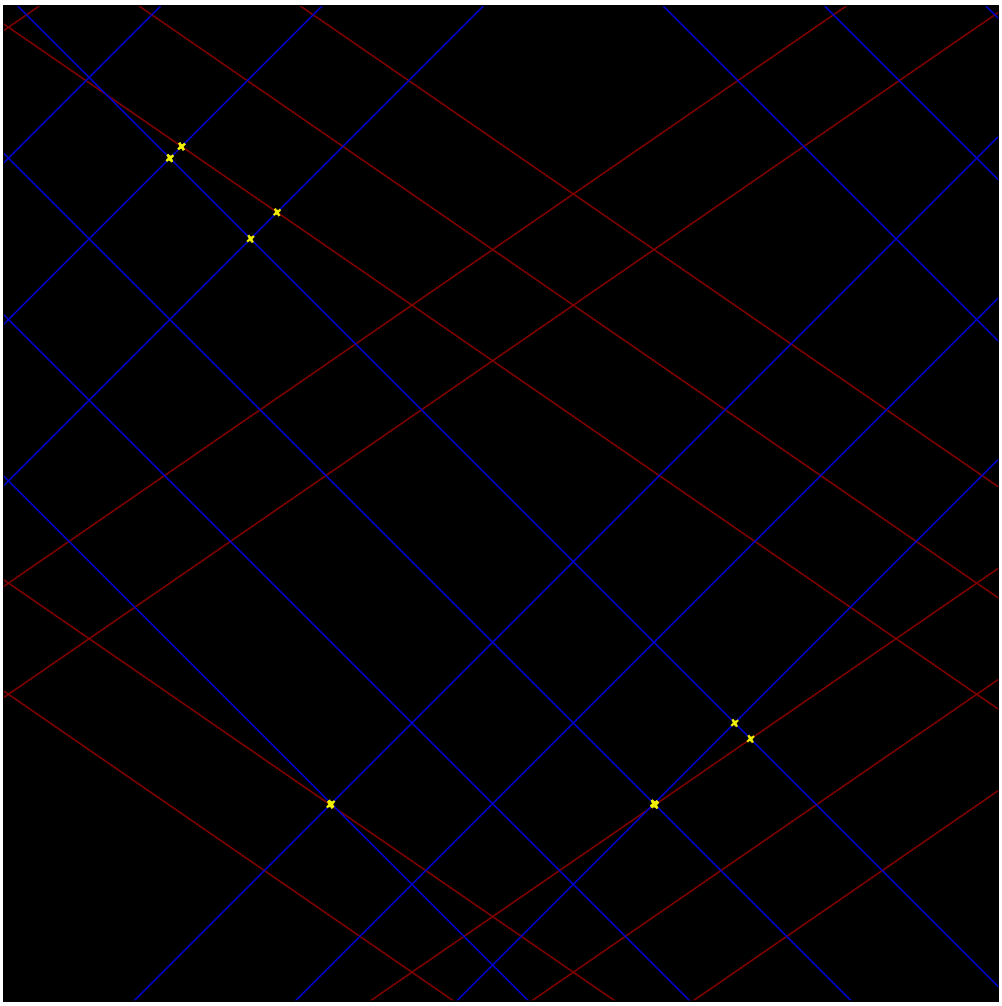

Figure 3.3: The Decorations for $\mathcal{U}$.

Figure 3.4 shows part of $\mathcal{U}(\theta; A)$ when $\theta = (1/11, 1)$ and $A = 4/11$. We have shown several orbits, using different colors. All vertices in sight are undecorated.

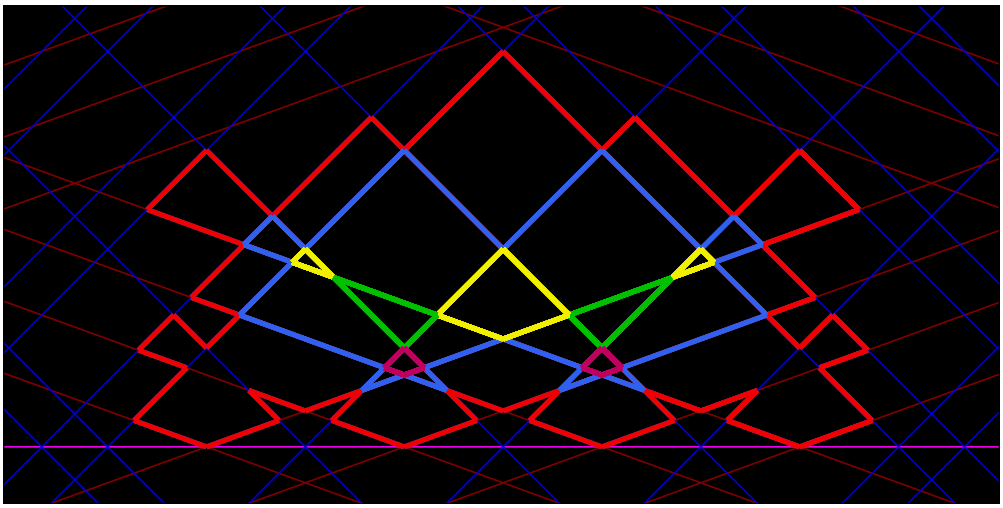

Figure 3.4: Some multigrid orbits for $\theta = (1/11, 1)$ and $A = 4/11$.

Figure 3.4 shows part of $\mathcal{U}(\theta; A)$ when $\theta = (1/72, 1)$ and $A = 17/72$. This time we show a single orbit of the multigrid flow. All vertices in sight are undecorated.

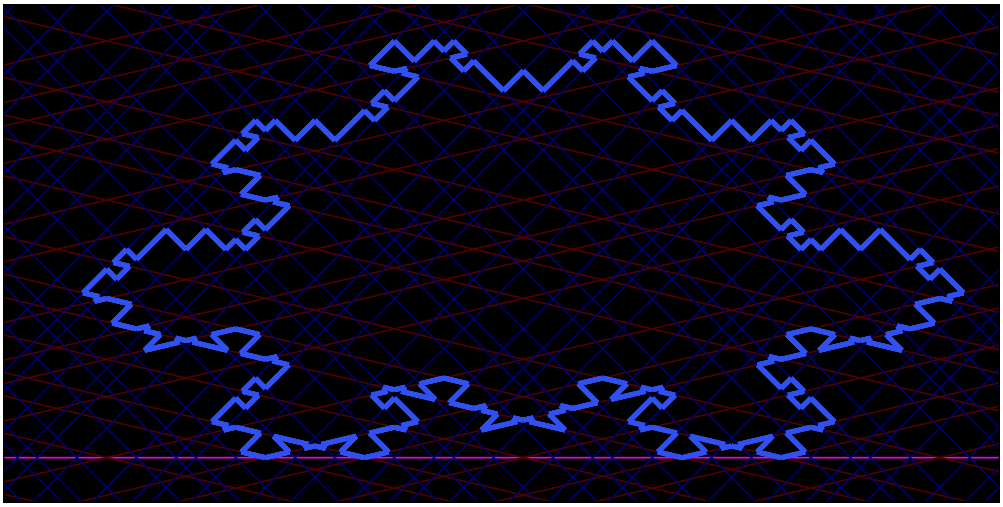

Figure 3.5: A multigrid orbit for $\theta = (1/72, 1)$ and $A = 17/72$.

Now we compare Figures 2.3 and 3.5. The coordinates we use for the arithmetic graph do not quite line up with the coordinates we use for our multigrid. Define

$$M = \begin{bmatrix} 1 & 1 \\ -A & B \end{bmatrix}; \qquad B = 1 + \frac{1}{2A} - \frac{A}{2}. \tag{10}$$

Here M maps the x-axis to the line of slope $-A$ through the origin.

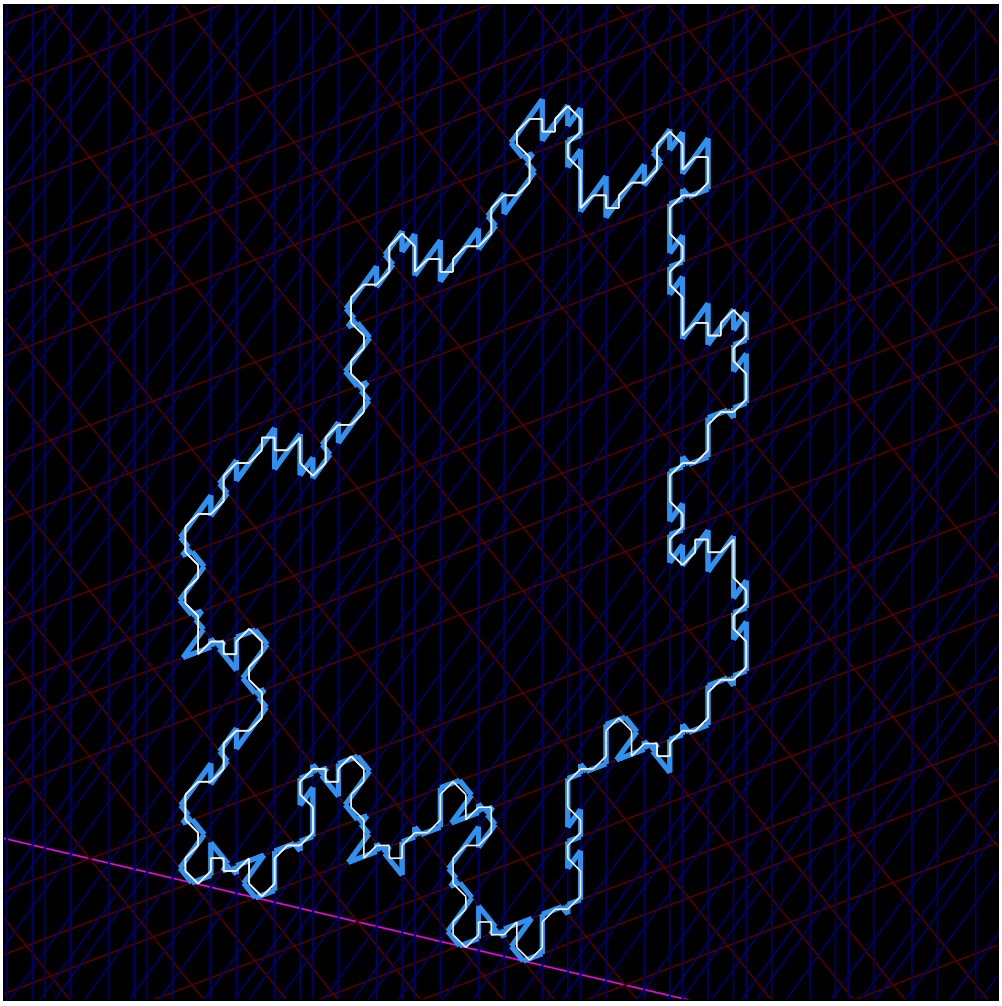

Figure 3.6: Figures 2.3 and 3.5 properly compared.

Here we plot $\Gamma(1, 17/72)$, the orbit from Figure 2.3, against the image of the orbit in Figure 3.5 under M. The former is shown in white and the latter is shown in blue. Notice the close matchup. Figure 3.7 shows a closeup of the picture, so that the reader can see the orbits better.

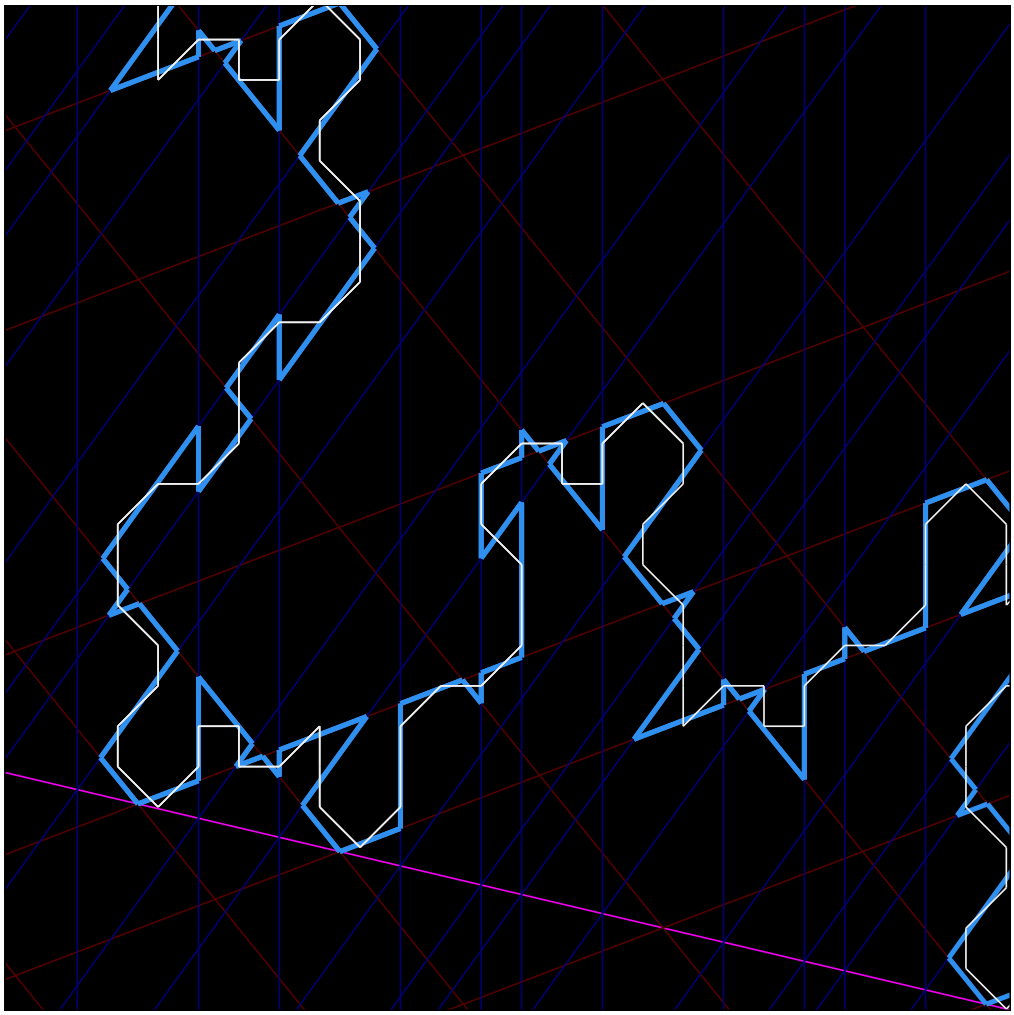

Figure 3.7: A Close-up of Figure 4.1.

These last two figures illustrate the Coarse Isomorphism Theorem.

4 The Coarse Isomorphism Theorem

4.1 Nearly Embedded Polygons

We say that a polygon $P \subset \boldsymbol{R}^2$ is *nearly embedded* if P is the limit of embedded polygons. Just to fix ideas, we insist that P has only finitely many double points. Figure 4.1 shows a picture of a nearly embedded polygon. We want to consider the case when P is either a closed polygon, or else an infinite polygonal arc. In the latter case, we assume that P is properly embedded: every compact subset of $\boldsymbol{R}^2$ intersects only finitely many segments of P. The multigrid orbits considered in the previous chapter serve as good examples of nearly embedded polygons.

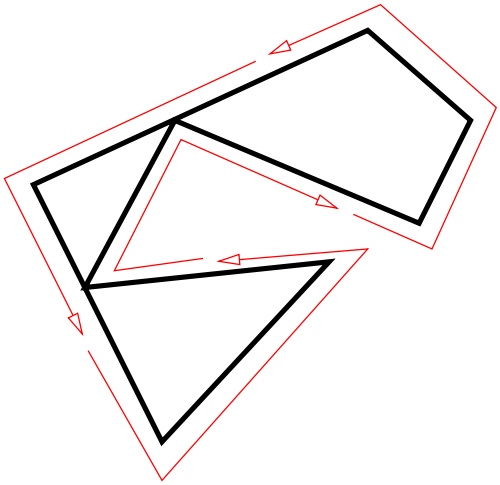

Figure 4.1: A good parametrization of a nearly embedded polygon.

We say that a *good parametrization* of a nearly embedded polygon P is a parametrization that is the limit of parametrizations of embedded polygons. The read arrows in Figure 4.1 suggest a good parametrization for the example shown. The parametrization of the multrigrid orbits that comes from the dynamics is a good parametrization. When P is closed, we think of the circle S^1 as the domain for the parametrization. When P is open, we think of $\boldsymbol{R}$ as the domain of the parametrization.

Let P_1 and P_2 be nearly embedded polygons. We consider the closed case first. We say that P_1 and P_2 are K-*close* if there are good parametrizations $f_k : S^1 \to P_k$ such that $\|f_1(t) - f_2(t)\| \le K$ for all $t \in S^1$. When P_1 and P_2 are open, we make the same definition with $\boldsymbol{R}$ in place of S^1.

4.2 The Coarse Isomorphism Theorem

We say that a *polygonal union* is a union $\mathcal{C}$ of nearly embedded polygons in the plane. We assume that $\mathcal{C}$ is locally finite, in the sense that only finitely many members of $\mathcal{C}$ intersect any given compact subset of $\boldsymbol{R}^2$. We say that a *stabilization* of $\mathcal{C}$ is a union of the form $\mathcal{C}' = \mathcal{C} \cup X$ where X is a discrete set of points.

We say that two polygonal unions $\mathcal{C}_1$ and $\mathcal{C}_2$ are *C-coarsely equivalent* if there are stabilizations $\mathcal{C}_1'$ and $\mathcal{C}_2'$ of $\mathcal{C}_1$ and $\mathcal{C}_2$ respectively, and a bijection $\phi : \mathcal{C}_1' \to \mathcal{C}_2'$ (between members of the two unions) such that correponding members of the two families are C-close.

Recall that M is the linear transformation defined in Equation 10.

Theorem 4.1 (Coarse Isomorphism I) *Let $A \in (0,1) - \boldsymbol{Q}$ be arbitrary. Let $\theta \in [0,2] \times [0,1]$ be such that the arithmetic graph $\Gamma(\theta; A)$ is entirely defined, and the multigrid $\mathcal{U}(\theta; A)$ is in general position. Then the union of components of $\Gamma(\theta; A)$ is C_A-coarsely equivalent to the union of orbits of the multigrid flow on $M(\mathcal{U}(\theta; A))$. The constant C_A only depends on A. The function $A \to C_A$ is uniformly bounded on $(\epsilon, 1-\epsilon)$ for any $\epsilon > 0$.*

The Coarse Isomorphism Theorem says that there is a bijection between the sufficiently long components of the arithmetic graph and the sufficiently long orbits of the multigrid flow. This bijection breaks down for very short orbits, and the device of stabilization is a succinct way of dealing with the issue. One can see from pictures that the bijection only breaks down for orbits whose diameter is less than about 5 units.

For the purpose of studying the large scale structure of the arithmetic graph (and hence of outer billiards on kites) the coarse equivalence given by the Coarse Isomorphism Theorem is just about exactly what we want. The dependence of the constant C_A on the parameter is annoying. We discuss this next.

As $A \to 0$ or $A \to 1$, the best constant C_A really does tend to ∞. However, the mismatch between the multigrid orbits and the arithmetic graph orbits is caused by a very simple mechanism that we might call *spike formation*. (See the figures below.) We can slightly modify our multigrid orbits and produce a uniform constant. Say that one polygon P' is a *truncation* of another polygon P if P' is obtained from P by replacing some consecutive pairs of edges of P with single edges. Figure 4.2 shows what we have in mind. The red dots indicate where we have made the changes.

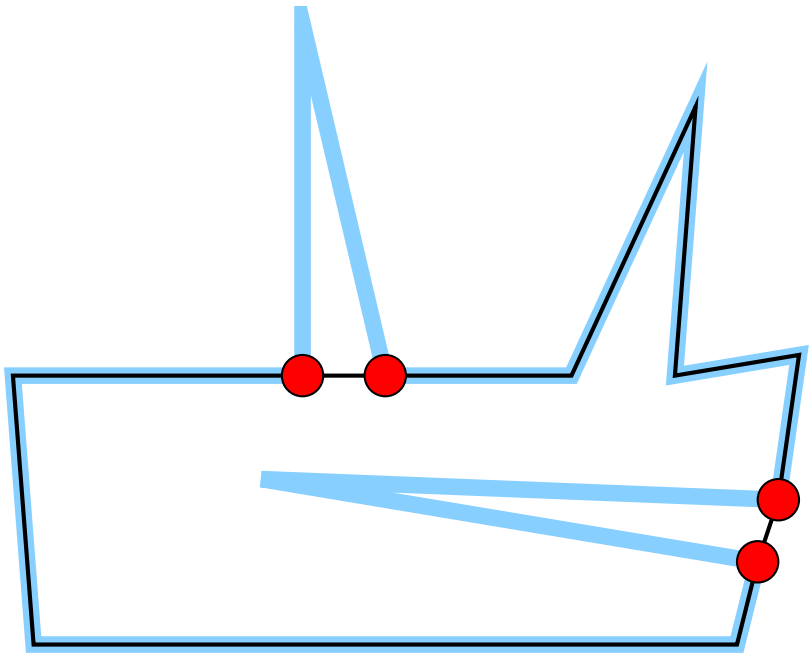

Figure 4.2: A blue polygon and its black truncation.

Here is a sharper version of the Coarse Separation Theorem. In this result, we think that the constant C is about 5.

Theorem 4.2 (Coarse Isomorphism II) *Let $A \in (0,1) - \boldsymbol{Q}$ be arbitrary. Let $\theta \in [0,2] \times [0,1]$ be such that the arithmetic graph $\Gamma(\theta; A)$ is entirely defined, and the multigrid $\mathcal{U}(\theta; A)$ is in general position. Then the union of components of $\Gamma(\theta; A)$ is C-coarsely equivalent to the union of suitably truncated orbits of the multigrid flow on $M(\mathcal{U}(\theta; A))$. The constant C is uniform.*

The general position requirement on $\mathcal{U}(\theta; A)$ is not really necessary for the Coarse Isomorphism Theorem. However, various complications make the theorem a bit trickier to state. However, even as stated, our result tells almost the whole story. For each choice of A, the is just a 1-dimensional subset of choices of θ for which our results do not apply.

In the next section we will show some pictures of the Coarse Isomorphism Theorem in action.

4.3 Some Pictures

The Coarse Isomorphism Theorem is most obvious when the temperature of the graph is low. Here we show an example when the temperature is 8/55. The multigrid orbit is shown blue and the arithmetic graph component is shown in white.

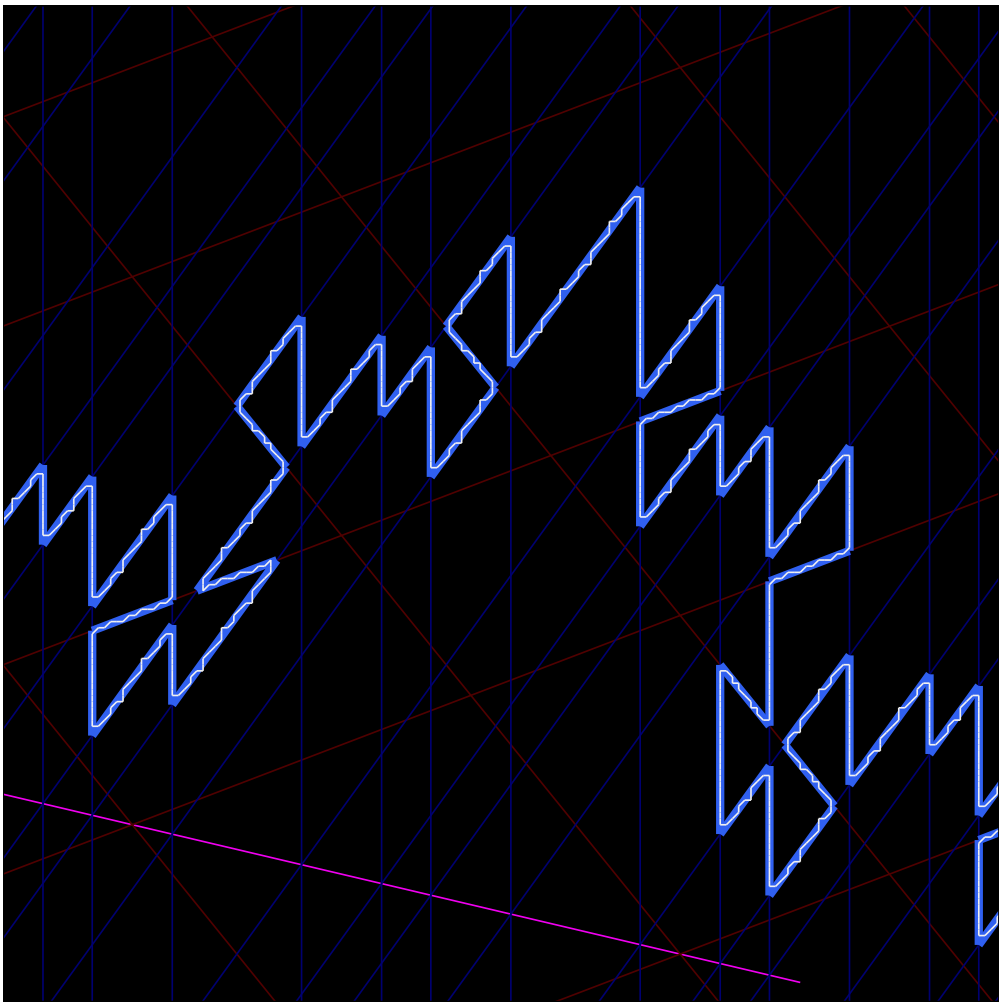

Figure 4.3: $A = 17/72$ and $\theta = (1/72, 8/55)$.

Figure 4.4 shows a picture at temperature 1. One sees this sort of space-filling behavior when the parameter is a good approximation to 1/2. Notice that there are certain spikes in the figure where the multigrid orbit deviates from the arithmetic graph component.

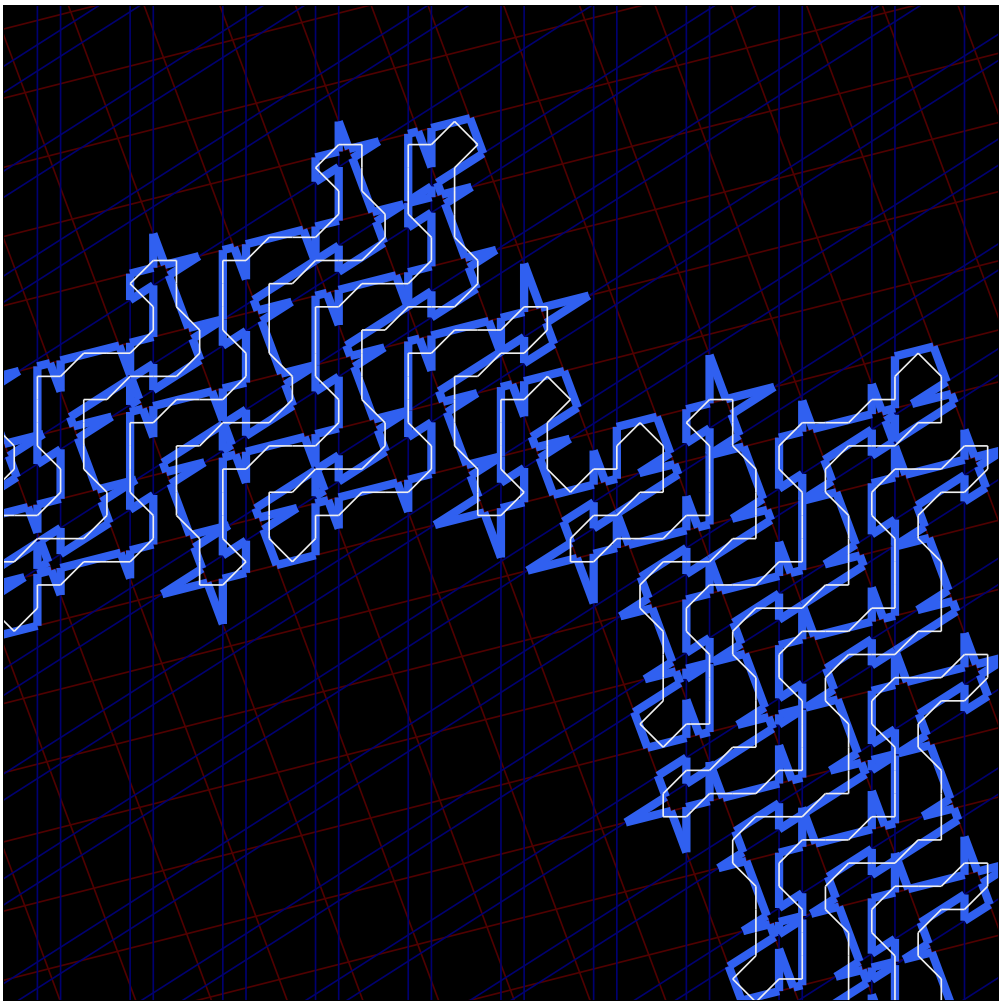

Figure 4.4: $A = 33/67$ and $\theta = (1/67, 1)$.

Figure 4.5 shows a more dramatic instance of the spiking phenomenon. Here the parameter A is quite close to 1. The second version of our Coarse Isomorphism Theorem is meant to deal with precisely this phenomenon. We get a much better approximation if we simply truncate all these spikes.

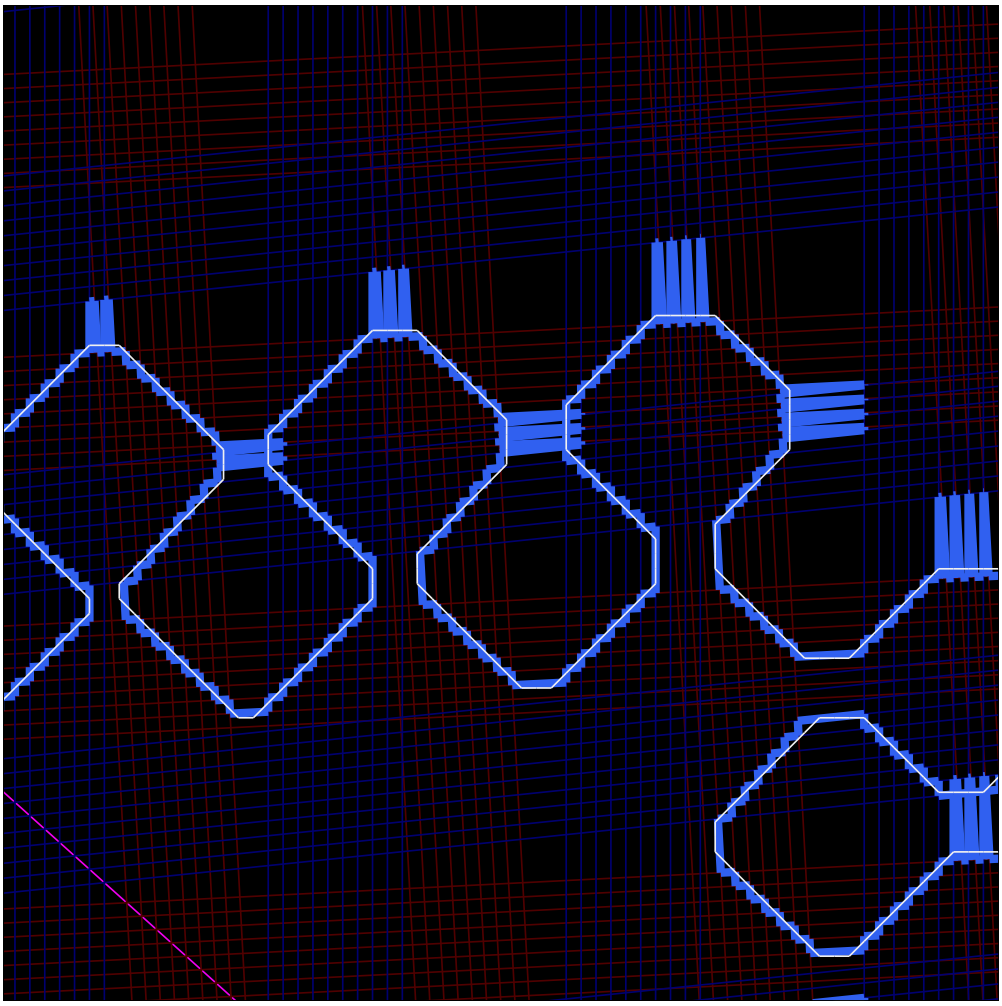

Figure 4.5: $A = 231/257$ and $\theta = (1/257, 1)$.

Finally, we end with a large component of an example we selected at random.

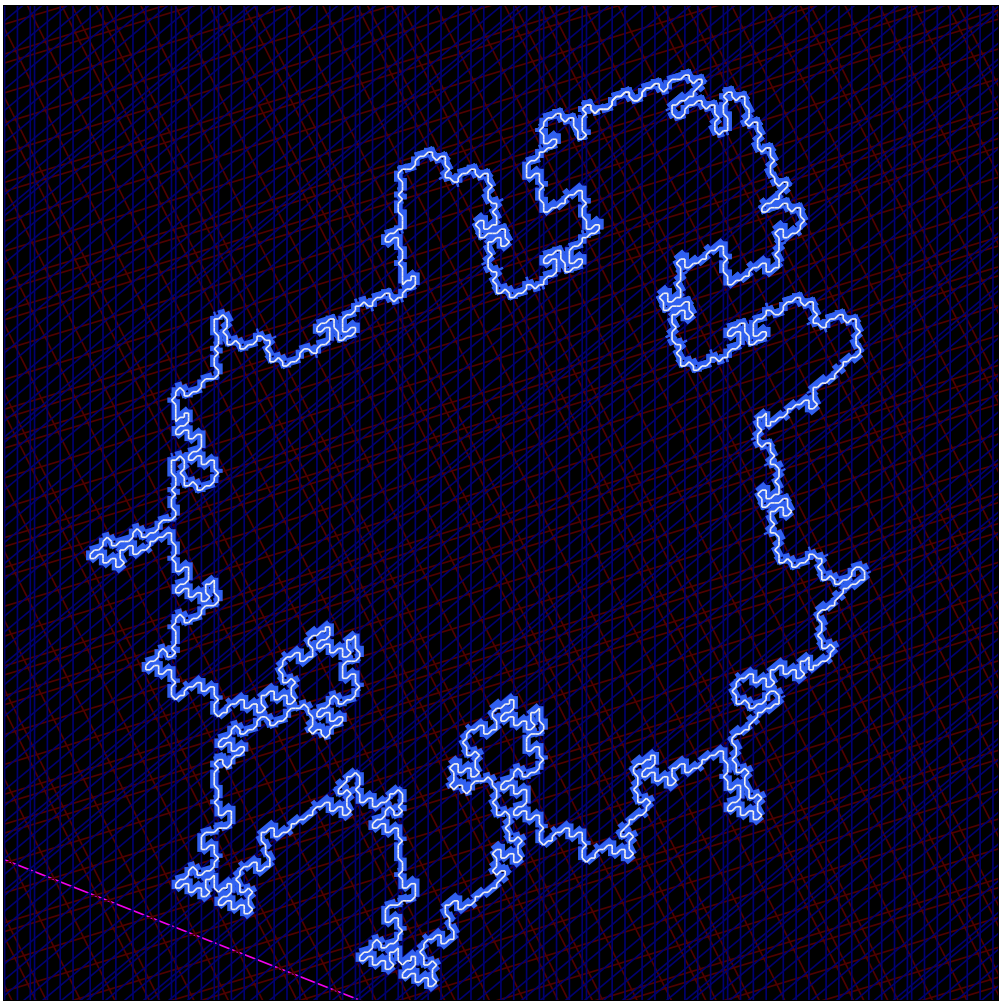

Figure 4.8: $A = 66/167$ and $\theta = (662/977, 355/523)$.

5 References

[**S1**] R. E. Schwartz, *Unbounded Orbits for Outer Billiards*, Journal of Modern Dynamics **3** (2007)

[**S2**] R. E. Schwartz, *Outer Billiards on Kites*, Annals of Mathematics Studies (2008) to appear.